Published in final edited form as:
J Comp Neurol. 2000 May 8; 420(3): 305–323.

Immunocytochemical Distribution of Corticotropin-Releasing Hormone Receptor Type-1 (CRF_1)-Like Immunoreactivity in the Mouse Brain: Light Microscopy Analysis Using an Antibody Directed Against the C-Terminus

Yuncai Chen[1,2], **Kristen L. Brunson**[1], **Marianne B. Müller**[3], **Wayna Cariaga**[1], and **Tallie Z. Baram**[1,2,*]

[1]Departments of Anatomy and Neurobiology, University of California at Irvine, Irvine, California 92697-4475

[2]Department of Pediatrics, University of California at Irvine, Irvine, California 92697-4475

[3]Max Planck Institute of Psychiatry, 80804 Munich, Germany

Abstract

Corticotropin-releasing hormone (CRH) receptor type 1 (CRF_1) is a member of the receptor family mediating the effects of CRH, a critical neuromediator of stress-related endocrine, autonomic, and behavioral responses. The detailed organization and fine localization of CRF_1-like immunoreactivity (CRF_1-LI) containing neurons in the rodent have not been described, and is important to better define the functions of this receptor. Here we characterize in detail the neuroanatomical distribution of CRF_1-immunoreactive (CRF_1-ir) neurons in the mouse brain, using an antiserum directed against the C-terminus of the receptor. We show that CRF_1-LI is abundantly yet selectively expressed, and its localization generally overlaps the target regions of CRH-expressing projections and the established distribution of CRF_1 mRNA, with several intriguing exceptions. The most intensely CRF_1-LI-labeled neurons are found in discrete neuronal systems, i.e., hypothalamic nuclei (paraventricular, supraoptic, and arcuate), major cholinergic and monoaminergic cell groups, and specific sensory relay and association thalamic nuclei. Pyramidal neurons in neocortex and magnocellular cells in basal amygdaloid nucleus are also intensely CRF_1-ir. Finally, intense CRF_1-LI is evident in brainstem auditory associated nuclei and several cranial nerves nuclei, as well as in cerebellar Purkinje cells. In addition to their regional specificity, CRF_1-LI-labeled neurons are characterized by discrete patterns of the intracellular distribution of the immunoreaction product. While generally membrane associated, CRF_1-LI may be classified as granular, punctate, or homogenous deposits, consistent with differential membrane localization. The selective distribution and morphological diversity of CRF_1-ir neurons suggest that CRF_1 may mediate distinct functions in different regions of the mouse brain.

Indexing terms

CRH; CRF; CRF-R1; rodent; immunocytochemistry; central nervous system

Corticotropin-releasing hormone (CRH), a 41-amino acid neuropeptide, is the primary hypothalamic factor involved in controlling the synthesis and release of adrenocorticotropic

*Correspondence to: Tallie Z. Baram, MD, PhD, Departments of Anatomy/Neurobiology and Pediatrics, University of California at Irvine, Irvine, CA 92697-4475. tallie@uci.edu.

hormone (ACTH) from the anterior pituitary (Vale et al., 1981). A large body of evidence indicates that CRH acts as a physiological mediator of stress-related functions (Aldenhoff et al., 1983; Ehlers et al., 1983; Siggins et al., 1985; Swanson et al., 1986; Conti and Foote, 1995; Sawchenko et al., 1996; Baram and Hatalski, 1998). CRH has also been demonstrated to be widely distributed throughout the brain (Swanson et al., 1983; Sawchenko and Swanson, 1985; Imaki et al., 1991; Sawchenko et al., 1993). In several regions, the peptide has been shown to have many of the physiological characteristics of a neurotransmitter (Young et al., 1986; Powers et al., 1987; Valentino and Wehby, 1988; Sawchenko et al., 1993).

The actions of CRH are mediated via interaction with distinct CRH receptors (Grigoriadis et al., 1996). Two general members of the CRH receptor family are currently known and consist of membrane-spanning G-protein-coupled molecules. The first, CRF_1 (or CRF-R1), has been cloned and functionally characterized in a number of species (Chang et al.,1993; Chen et al., 1993; Perrin et al., 1993; Palchaudhuri et al., 1998). This receptor binds CRH with high affinity and is positively linked to adenylate cyclase. Rat CRF_1 is found in the pituitary and the central nervous system (CNS) and is the candidate mediator for many of the neuroendocrine and neuromodulatory effects of CRH (De Souza et al., 1985; Potter et al., 1994; Chalmers et al., 1995; Baram et al., 1997; Radulovic et al., 1998). The amino acid sequence of mouse CRF_1 is highly similar to that of rat CRF_1 (Vita et al., 1993). However, recently, Radulovic et al. (1998) showed that CRF_1 is differently glycosylated in rat and mouse, as indicated by a higher molecular weight of mouse CRF_1 protein. These authors, using Western blotting, also suggested that the mouse CRF_1 may not share the regional brain distribution of the rat receptor. The second receptor, CRF_2, is found in at least three subtypes in human and rat ($CRF_{2\alpha}$, $CRF_{2\beta}$, and $CRF_{2\gamma}$), one of which, $CRF_{2\alpha}$ is found primarily in the CNS (Lovenberg et al., 1995; Kostich et al., 1998).

The distributions of messenger RNAs (mRNAs) of the two CRH receptors in rat brain have been demonstrated using in situ hybridization. Thus, Potter et al. (1994) and Chalmers et al. (1995) described, respectively, the anatomical distribution of CRF_1 mRNA and CRF_2 mRNA in adult rat brain, demonstrating distinct patterns for each of these receptors. Also, significant differences in CRH receptor mRNA distribution have been described in different species (Sanchez et al., 1999). Importantly, the detailed organization and the fine localization of CRF_1 in rodent brain have not been delineated. In addition, mRNA analysis does not provide information about the intracellular localization of CRF_1 to somata versus processes, or about clustering and synaptic relationships of receptor molecules. Therefore, the goal of the present study was to utilize immunocytochemical methods to provide a detailed, single-cell-resolution description of the distribution of CRF_1 in the mouse brain.

MATERIALS AND METHODS

Animals

Adult male C57 black mice (2 months old) were used in this study. Because the overall goals of this series of studies included understanding the possible regulation of CRF_1 by its ligand, CRH, care was taken to utilize mice of similar genetic make-up in all stages of this effort. Therefore, mice used here were progeny of breeding pairs heterozygous for a null CRH allele (a generous gift from Dr. J Majzoub). Specifically, transgenic mice in whom an allele of the CRH gene has been replaced with a neomyocin resistance gene were crossed back to the C57 background strain for a minimum of 14 generations. Progeny of heterozygous breeding pairs were genotyped by polymerase chain reaction analysis (Muglia et al., 1995), and those found to possess both alleles of the CRH gene (wild type) were used in this study.

To account for potential variation in CRF_1 distribution or abundance deriving from the specific strain or genetic make-up of these mice, brains from two additional mice from a separate strain (129/Ola or CD1 strain) were also studied, with essentially indistinguishable results (not shown). Mice were born and maintained in a federally approved animal facility, and litter size was culled to six. Mice were kept on a 12-hour light/dark cycle and given free access to food and water. All experiments were carried out according to NIH guidelines for the care of experimental animals, with approval by the institutional animal care committee.

Antiserum generation

A polyclonal anti-CRF_1 antiserum was generated in goat, against a 20-amino acid peptide sequence (Santa Cruz Biotechnology, Santa Cruz, CA). The synthetic peptide antigen, comprising the C-terminus of CRF_1 (SIPTSPTRVSFHSIKQSTAL), corresponds to amino acids 425–444 of human CRF_1 and is identical with amino acids 396–415 of mouse and rat CRF_1. This sequence differs by three amino acids from the corresponding portion (412–431) of mouse CRF_2. A search of GenBank and SwissProt data bases revealed no known sequences (aside from CRH receptors of other species) with significant homology to this portion of the CRF_1 receptor. To characterize the antigen interacting with the antiserum further, Western blotting was also carried out. To determine whether cross-reactivity with the CRF_2 receptor occurred at the dilution used in this study (as suggested by the manufacturer), sections of mouse heart, known to express only the CRF_2 receptor, were subjected to immunocytochemistry in parallel with brain sections.

Western blotting

Brains were rapidly dissected from adult mice of two strains that were killed by decapitation. The hypothalamus and cerebellum were then separated carefully and homogenized in 50 mM Tris-HCl (pH 7.4, 4°C) containing 150 mM NaCl, 0.25% sodium dodecyl sulfate (SDS), 0.25% sodium deoxycholate, 1 mM EDTA, 2 μg/ml aprotinin, 2 μg/ml leupeptin, and 2 μg/ml pepstatin. The crude extracts were centrifuged at 14,000 rpm for 20 minutes at 4°C. The supernatant was collected and centrifuged for 10 minutes. The clear supernatant fluid (containing soluble proteins and membrane fraction) was then collected for the following analysis. Protein concentration was determined using BCA Protein Assay (Pierce, Rockford, IL), and 50-μg protein aliquots were size-fractionated on 4–12% Tris-glycine gel (Novex, Carlsbad, CA) at 120 V for 2.5 hours.

After electrophoresis, proteins were transferred to Hybond-ECL membrane (Amersham, Arlington Heights, IL). Nonfat milk (6%) in Tris-buffered saline (25 mM Tris, 0.15 M NaCl, pH 7.2) containing 0.05% Tween-20 (TBS-T) was used for blocking and for dilution of primary and secondary antibodies. The membrane was blocked overnight at 4°C and then incubated for 2 hours at room temperature with the anti-CRF_1 antiserum (1:500). After several washes with TBS-T, the membrane was incubated in horseradish peroxidase-conjugated anti-goat IgG (1:10,000, Jackson ImmunoResearch, West Grove, PA) for 1.5 hours at room temperature. Following rinsing with TBS-T, bound antibody was detected using the ECL detection system (Amersham). For control, the primary antiserum was preadsorbed overnight at 4°C with purified CRF_1 blocking peptide (100 μg/ml; Santa Cruz Biotechnology).

Immunocytochemistry

Care was taken to harvest tissue under relatively stress-free conditions (Yan et al., 1998a,b). Briefly, mice (n = 4) were undisturbed for at least 24 hours prior to experiments and then deeply anesthetized with sodium pentobarbital (100 mg/kg intraperitoneally) within 45 seconds of initial handling. Mice were then removed to the laboratory and perfused via the ascending aorta with 0.9% saline solution followed by freshly prepared 4%

paraformaldehyde in 0.1 M sodium phosphate buffer (PB, pH 7.4, 4°C). Brains were dissected from the skull, postfixed for 4 hours, and immersed in 15%, followed by 25% sucrose for cryoprotection. Brains were blocked in the coronal or sagittal planes and sectioned at 20-μm thickness using a cryostat. In each plane, one in eight matched sections (one in four for the hypothalamic region) were subjected to immunocytochemistry, and an adjacent series of sections was stained with cresyl violet.

For CRF_1-LI immunocytochemistry, free-floating sections were collected into tissue-culture wells in 0.1 M PB and subjected to standard avidin-biotin complex (ABC) methods (Chen et al., 1998a; Yan et al., 1998a,b). Briefly, after several washes with 0.01 M phosphate-buffered saline (PBS) containing 0.3% Triton X-100 (pH 7.4, PBS-T), sections were treated for 30 minutes in 0.3% H_2O_2 in PBS, followed by blockade of nonspecific sites with 2% normal rabbit serum in PBS for 30 minutes. After a 10-minute rinse in PBS, sections were incubated for 48 hours at 4°C with anti-CRF_1 (1:5,000) in PBS containing 1% bovine serum albumin and 2% normal rabbit serum and washed 3 times in PBS-T, 5 minutes each. Subsequently, sections were incubated in biotinylated rabbit-anti-goat IgG (1: 200, Vector, Burlingame, CA) in PBS for 1 hour at room temperature. After washing in PBS-T (3 × 5 minutes), sections were incubated in ABC solution (1:100; Vector) for 2 hours at room temperature. Sections were then rinsed again in PBS-T (3 × 5 minutes). The reaction product was visualized by incubating sections for 8–10 minutes in 0.04% 3,3′-diaminobenzidine (DAB) containing 0.01% H_2O_2 with or without 0.5% nickel chloride.

Several approaches were used to address the specificity of the immunostaining obtained with anti-CRF_1. In addition to the Western blotting described above, the specificity of the primary antiserum was also tested by substituting normal goat IgG (1:1,000–5,000; Santa Cruz Biotechnology) for the primary antiserum and by preadsorbing the antiserum overnight with purified CRF_1 blocking peptide (100 μg/ml). The specificity of the second antibody was tested by omitting the primary antiserum during the first incubation. As indicated above, cross-reactivity with CRF_2 was tested by using the antiserum for staining mouse heart tissue, known to express CRF_2 only.

Regional and laminar distribution patterns of CRF_1-LI were determined by comparison of immunocytochemical sections with adjacent cresyl-violet stained sections and by evaluation of methyl green-counterstained sections. Published nomenclature was used to identify cytoarchitectonic areas in the cortex (Dolorfo and Amaral, 1998), amygdala (Pitkänen et al., 1997), hypothalamic paraventricular nucleus (Swanson and Kuypers, 1980; Swanson et al., 1983), and other regions (Sidman et al., 1971; Paxinos and Watson, 1982).

Density and intensity of CRF_1-LI-labeled neurons

The relative density of CRF_1-ir neurons was assessed with a square lattice system (Chen et al., 1998b) over the entire area examined, using light microscopy at ×400 magnification. Density was expressed as the percentage of positive cells related to total cell number in the region of interest or in a 0.01-mm^2 real area, based on the average value from three fields per section. Generally, three to five sections were counted in every mouse for evaluating CRF_1-ir neuronal density in each brain structure or nucleus, and the percentage of CRF_1-ir neurons was calculated by dividing the total number of CRF_1-ir neurons by the sum of Nissl-stained cells. The intensity of CRF_1-LI labeling was scored as weak (+), moderate (++), intense (+++), or strongly intense (++++).

RESULTS

The specificity of the anti-CRF_1 antiserum was assessed by immunoblotting mouse hypothalamus and cerebellum homogenates (Fig. 1). As shown in lanes 1 and 2, the

antiserum recognized an approximately 80-kDa protein, in good agreement with the molecular weight of mouse brain CRF_1 protein (Radulovic et al., 1998). Preadsorption of the primary antiserum with a blocking peptide consisting of the immunogenic epitope (100 μg/ml) completely abolished the CRF_1 band (Fig. 1, lanes 3 and 4). The specificity of CRF_1 immunoreactivity was also indicated by the absence of labeled neurons or fibers in brain sections that were stained using antiserum pretreated with the antigenic peptide (Fig. 2D). In addition, no staining was observed on the sections when normal goat IgG was substituted for the CRF_1-directed serum or in the absence of the primary antiserum (not shown). Finally, cross-reactivity with the CRF_2 receptor was excluded by the absence of any signal in mouse heart specimens run in parallel to immunopositive brain sections (not shown).

CRF_1-LI neurons were widely but selectively distributed throughout the mouse brain. In addition, the intensity of CRF_1 reaction product in positive neurons differed in a neuron- and region-specific manner. In general (but not always; see Fig. 2C), CRF_1-LI in most involved brain regions showed a pattern typical of membrane localization and was further characterized as either granular (associated with intensely labeled neurons) or finely punctate (generally present in moderately or weakly labeled cells). A third pattern, a homogenous deposit associated with the plasma membrane, was found in several regions (Fig. 2A–C). Notably, intensity of the CRF_1 immunoreaction product was maximal in neocortical pyramidal cells, Purkinje cells, and most positive neurons in the thalamus, hypothalamus, and brainstem nuclei.

The distribution of CRF_1-LI neurons in the four mouse brains studied in detail was essentially identical, with relatively modest variation in labeling intensity among animals. The following is a description of the distribution of CRF_1-LI neurons by region.

Telencephalon

Table 1 outlines the distribution of CRF_1-LI in the telencephalon.

Olfactory bulb and tubercle—In the olfactory bulb (Fig. 3A), many periglomerular cells were intensely CRF_1-LI labeled and thus outlined the glomeruli that were unstained. In addition, a few large, multipolar, intensely labeled neurons were observed just beneath the glomerular layer. Mitral cells were moderately or weakly immunoreactive, and some weakly labeled neurons were also present in the external and internal plexiform layers. In addition, some immunoreactive puncta were observed in the internal plexiform layer and, rarely, in the external plexiform layer. The granular layer contained numerous labeled puncta and scattered CRF_1-LI neurons. The distribution pattern of CRF_1-LI in the accessory olfactory bulb resembled that found in the main bulb; conversely, most neurons in the anterior olfactory nucleus were CRF_1-ir. Within the olfactory tubercle (Fig. 3B), moderately CRF_1-LI-labeled neurons were prominent in the pyramidal layer. Scattered large, multipolar, intensely labeled neurons and some medium-size, weakly labeled cells were seen in the polymorphic layer, but none in the plexiform layer. The islands of Calleja contained moderately labeled CRF_1 granular reaction products, whereas neurons in the taenia tecta were moderately immunoreactive.

Cerebral cortex—Neocortical areas contained a large number of CRF_1-LI neurons, the intensity of which differed substantially across regions. The most intensely labeled neurons occurred in the cingulate cortex and in the somatosensory area of the frontoparietal cortex, followed by the motor area of frontoparietal cortex. CRF_1-LI neurons in the association areas of the striate and temporal cortices were characterized by moderately intense reaction product. The laminar distribution of CRF_1-LI-labeled neurons was striking: in the cingulate, frontoparietal, and most other neocortical regions, whereas immunopositive neurons were

distributed throughout layers II–VI, maximal intensity of the reaction product was found in layer V, most notably in the frontoparietal cortex motor area (Fig. 3C). In addition, rare CRF_1-LI neurons were observed in layer I and in subcortical white matter. Within piriform cortex, moderately labeled CRF_1-ir neurons were common in both the pyramidal (II) and polymorphic (III) layers, intermingled with a smaller population of intensely labeled cells (Fig. 3D). In the entorhinal cortex, many moderately labeled neurons were distributed in layers II and III, accompanied by a scattered population of large, multipolar, intensely labeled neurons. CRF_1-LI neurons in layers V–VI were moderately labeled (Fig. 3E). Perirhinal cortex contained CRF_1-LI-labeled neurons uniformly throughout layers II and III.

Hippocampal formation—Within the hippocampus, CRF_1-LI-containing neurons were most prominent in the pyramidal cell layer: the CA1 pyramidal cell layer was rich in moderately labeled puncta and contained several intensely labeled large neurons. CA2 was distinguished by intense or moderate labeling of virtually all pyramidal neurons. In CA3, maximal intensity of CRF_1-ir was found in CA3a, with a gradual decline over CA3b and a fainter signal over CA3c. Outside the pyramidal layer, only occasional medium-sized, multipolar or fusiform CRF_1-ir neurons were scattered in the strata oriens, lacunosum-moleculare, and radiatum (Fig. 4A,B). Within the dentate gyrus, granule cell somata were outlined by a fine mesh of weakly stained puncta, and occasional strongly labeled basket-like neurons were visible. Large, polymorphic, intensely labeled neurons were present in the hilus, whereas little CRF_1-LI was observed in the molecular layer (Fig. 4A,C). Within the subiculum, many pyramidal neurons were intensely labeled (Fig. 4D).

Amygdala—Large, intensely labeled neurons were widely distributed throughout the basal nucleus (Fig. 5A,B). The staining pattern of the accessory basal nucleus consisted of weakly labeled medium-sized neurons, and this pattern was shared by the medial nucleus: in both nuclei, only a portion of the cell surface typically showed CRF_1-LI (Fig. 5C). Most neurons were immunoreactive in the anterior cortical nucleus, with a similar pattern but lower intensity than in the medial nucleus. In the central nucleus (ACe), weak to moderate CRF_1-LI labeling was found in both lateral and medial divisions, but with a different staining pattern: whereas immunoreactivity in the lateral division consisted of punctate deposits, the medial division pattern consisted of crescent-shaped contours (similar to the pattern found in medial and accessory basal nuclei; Fig. 5D). Finally, weakly labeled neurons were present in the lateral nucleus. Within the bed nucleus of stria terminalis (considered a part of the “extended amygdala”), moderately labeled puncta were abundant in both medial and lateral areas (not shown).

Basal forebrain—Most lateral septal nucleus neurons showed intense CRF_1-LI. Interestingly, each subnucleus demonstrated a distinct immunoreactivity pattern (Fig. 6A–C): the dorsal region contained many medium-size neurons with granular CRF_1-LI deposits (Fig. 6B), whereas the intermediate region also contained (medially) cells with a fine punctate CRF_1-LI pattern and short processes. A third pattern, consisting of large granular deposits without a distinct neuronal contour, was observed in the ventral region of this septal nucleus (Fig. 6C). The medial septum contained many large, intensely or moderately labeled neurons, whereas multipolar, intense CRF_1-LI-labeled magocellular neurons were abundant in both the horizontal and vertical limbs of the diagonal band of Broca (Fig. 6D).

Basal ganglia—Most CRF_1-LI neurons in the striatum (caudate-putamen) were weakly labeled and were accompanied by scattered medium-sized, intensely labeled cells (Fig. 6E). A similar but more intense labeling pattern was evident in the nucleus accumbens (Fig. 6F). The fundus striati and ventral endopiriform nucleus were characterized by abundant, moderately CRF_1-LI neurons. A population of larger, multipolar or fusiform process-

possessing neurons was encountered in the globus pallidus and the ventral pallidum (Fig. 6F), whereas the entopeduncular nucleus contained moderate numbers of intensely CRF_1-LI cells.

Diencephalon

Table 2 outlines the distribution of CRF_1-LI neurons in the diencephalon.

Habenula—Small neurons in medial habenula were intensely CRF_1-LI labeled, whereas lateral habenula showed numerous moderately CRF_1-LI neurons and scattered intensely labeled cells (Fig. 7A).

Thalamus—The anterior nuclear group demonstrated numerous CRF_1-LI strongly labeled neurons (in the anterodorsal and anteromedial nuclei) and moderately labeled ones (anteroventral nucleus) (Fig. 7A). Many neurons with intensely labeled somata and short processes were found in the mediodorsal nucleus. In the lateral nuclear group, the dorsal and posterior nuclei contained multipolar or triangular intensely CRF_1-LI neurons possessing short processes. In the ventral group, intensely labeled neurons were abundant in the lateral, posterolateral, and posteromedial nuclei, as well as in the midline nuclear group (paratenial, paraventricular, and reuniens nuclei) and in the intralaminar nuclear group. In the thalamic reticular nucleus, only weak or moderate CRF_1-LI was found (Fig. 7B).

Hypothalamus—Within hypothalamus, most CRF_1-LI labeling of neurons was intense, especially in the supraoptic, paraventricular (PVN), ventromedial (VMH), and arcuate nuclei (Fig. 8A–F). The medial preoptic area contained numerous highly CRF_1-LI neurons, reminiscent of those of the amygdaloid medial nucleus, whereas the lateral preoptic nucleus contained triangular or fusiform, moderately labeled cells bearing several short processes. The suprachiasmatic nucleus was characterized by densely immunoreactive neuropil, whereas the retrochias-matic area contained a few weakly CRF_1-LI-positive neurons in conjunction with scattered intensely CRF_1-LI-positive puncta. Neurons in the supraoptic nucleus were more strongly immunolabeled than those in the suprachiasmatic nucleus (Fig. 8D). Parvocellular neurons of the PVN demonstrated exceptionally strong CRF_1-LI; in contrast, few positive neurons were present in the magnocellular divisions (Fig. 8A–C). In the VMH, neurons were intensely labeled ventrolaterally and moderately labeled in the dorsomedial part, in a granular pattern. Intensity of CRF_1-ir in the arcuate nucleus was higher than that observed in the VMH (Fig. 8E,F). Staining intensity of CRF_1-LI in neurons of the posterior lateral hypothalamic area was mostly weak or moderate. Interestingly, several subependymal neurons in the median eminence showed CRF_1-LI (Fig. 8E).

Subthalamus and geniculate bodies—Subthalamic neurons showed CRF_1-LI, as did most zona incerta cells (Fig. 7C). In the lateral geniculate body, neurons were generally intensely labeled dorsally and moderately or weakly labeled in the ventral parts, whereas both parts of the medial geniculate body contained intensely immuno-reactive neurons.

Mesencephalon

Table 3 outlines the distribution of CRF_1-LI-expressing neurons in the mesencephalon. A large number of CRF_1-LI-labeled neurons was observed in the tectum. Within layers II–VII of the superior colliculus, these neurons were moderately or weakly immunoreactive, accompanied by a few large, multipolar, deeply labeled cells in the lateral part of layer VI and occasionally in layer VII (Fig. 9A). The most striking feature of the inferior colliculus was large, multipolar or triangular, strongly CRF_1-LI neurons in both the cortical and central nuclei, where most medium-sized neurons were moderately stained (Fig. 9B). Comparison

of the dorsal and lateral inferior colliculus cortex revealed a few CRF_1-LI neurons in the latter.

Within tegmental nuclei, labeling intensity was maximal in the ventral (Fig. 9C), moderate in the laterodorsal, and weak in the dorsal nucleus (Fig. 9C,G). Neurons in the pedunculo-pontine-tegmental and reticulotegmental nuclei were strongly labeled. In red nucleus, most large neurons with short processes were intensely labeled (Fig. 9D). The substantia nigra pars reticulata was characterized by large, multipolar, neurons with intense CRF_1-LI, whereas the pars compacta contained medium, moderately to intensely labeled cells (Fig. 9E). Similarly, process-bearing neurons in the interpeduncular nucleus were moderately or intensely labeled. The dorsal raphe nucleus was rich in highly labeled neurons, whereas only modest numbers of intensely stained neurons were observed in the median raphe (Fig. 9G).

Both the accessory (Edinger-Westphal) and principal oculomotor nuclei contained moderate or intense CRF_1-LI (Fig. 9F). Neurons with short processes in the Darkschewitsch nucleus were moderately labeled. The mesencephalic nucleus of the trigeminal nerve showed intense CRF-LI in a granular pattern (see Fig. 11A). In addition, many medium-sized, moderately labeled neurons were present in the central gray, particularly dorsally.

Pons and medulla

Pontine and medullary raphe nuclei shared the staining pattern of their mesencephalic counterparts. Within the reticular formation, large, multipolar, intense CRF_1-LI neurons were abundant in the pontine and gigantocellular reticular nuclei, whereas only scattered positive neurons resided in the intermediate and lateral nuclei. The locus coeruleus was rich in multipolar, intensely CRF_1-LI-labeled neurons (see Fig. 11A). Dorsal parabrachial nuclei were more intensely stained than ventral ones (see Fig. 11B). Large, multipolar neurons in superior olive and nuclei of lateral lemniscus were also intensely stained.

Within trigeminal nerve nuclei, large, multipolar neurons in the motor, principal sensory, and spinal subnuclei showed intense CRF_1-LI. In addition, numerous moderately labeled small and medium cells were found in both principal sensory and spinal nuclei (Fig. 10A). The facial nucleus was rich in large, multipolar CRF_1-LI neurons (Fig. 10B), whereas the vestibular nuclei (medial, lateral, and superior) contained numerous moderately or in-tensely labeled cells (Fig. 10C). In the cochlear complex, the ventral nucleus had more intense CRF_1-LI than the dorsal nucleus, the latter containing rare highly labeled neurons and some moderately immunoreactive neurons (Fig. 11C). Some neurons in vagal, ambiguous, and hypoglossal nuclei showed strong CRF_1-LI (Fig. 10D,E). Weak-to-moderate CRF_1-LI labeling occurred in medial and lateral divisions of the solitary tract nucleus (Fig. 10F).

Medium-sized, highly labeled CRF_1-LI neurons were observed in the medial nucleus of the trapezoid body, in contrast to the occasional, intensely labeled cells of the lateral nucleus (Fig. 11D,E). In the inferior olive, medium-sized CRF_1-LI-stained neurons were found (Fig. 11F).

Cerebellum

Purkinje cells showed intense CRF_1-LI, in a granular pattern (Figs. 2A, 11G), whereas the granular layer contained only scattered intensely labeled neurons accompanied by abundant weakly labeled puncta. Large, multipolar neurons in the deep cerebellar nuclei were intensely stained, whereas the cerebellar white matter was devoid of CRF_1-LI.

DISCUSSION

The current immunocytochemical study describes the distribution of CRF_1-LI throughout the mouse brain. The results indicate that 1) CRF_1-LI is generally localized to the cell membrane and is further characterized as granular, punctate, or homogenous deposits; 2) CRF_1-LI-labeled neurons are morphologically heterogeneous both within and among brain structures; 3) CRF_1-LI is widely and selectively distributed in discrete regions of the mouse brain, in a pattern that—with notable exceptions—generally conforms to that of CRF_1 mRNA; and 4) a gradient of CRF_1-LI labeling intensity exists, with the highest found in certain hypothalamic nuclei, neocortex, septum, basal amygdala, thalamus, select brain stem regions, and cerebellar Purkinje cells.

CRF_1 immunoreaction product was generally localized to the cell membrane. This result is consistent with evidence indicating that this receptor is a G-protein-coupled, membrane-bound protein (Chang et al., 1993; Perrin et al., 1993; Castro et al., 1996). Of the several patterns of CRF_1-LI observed in this study (Fig. 2A–C), some may signify receptor clustering (granular and punctate deposits). In addition, the spectrum of cellular distribution patterns of CRF_1-LI was remarkable, both within a given nucleus as well as among regions. Most commonly, punctate or granular CRF_1-LI outlined a neuronal profile consisting of the soma with or without dendritic processes. In some cases, CRF_1-LI outlined only part of the cell surface, suggesting somatic innervation, perhaps by a spatially discrete bundle of axons (e.g., the climbing fiber innervation of cerebellar molecular layer neurons). Interestingly, numerous CRF_1-LI-labeled puncta were observed in certain regions such as the granular layers of the olfactory bulb and cerebellum, suggesting a presynaptic location of CRF_1. Thus, the findings of this study are consistent with a potential for not only the post- but also presynaptic location of CRF_1. However, electron microscopic (EM) studies are required to demonstrate the presence of presynaptic CRF_1 definitely.

In general, neurons with CRF_1-LI were observed in target regions of CRH-expressing local circuit and projection neurons. An eloquent example of this notion was evident in the amygdala. In the ACe, CRH-containing terminals are abundant and have been shown to arise from cell bodies located in the lateral hypothalamus and dorsal raphe, as well as from intrinsic CRH neurons in the ACe (Swanson et al., 1983; Uryu et al., 1992). In the present study, we observed that essentially all ACe neurons were CRF_1-LI positive. This indicates that in the ACe, CRF_1-ir neurons may be innervated by CRH-expressing cells originating both within and outside the amygdala. Interestingly, the density and intensity of CRF_1-immunoreaction product in the ACe were high. In contrast, CRF_1 mRNA expression in the ACe has been found to be modest (Potter et al., 1994; Chalmers et al., 1995; Avishai-Eliner et al., 1996). Thus, it may be suggested that the CRF_1-LI in the ACe may originate in the somata of other nuclei (e.g., lateral amygdala; Pitkänen et al., 1997) and transported to ACe. An additional, intriguing possibility is that the ACe may contain novel, as yet uncharacterized, ligand for this receptor (e.g., Weninger et al., 1999). Whereas levels of CRF_1-LI and mRNA are somewhat discordant in the ACe, the results of the current study—showing intense labeling of magnocellular neurons in basal nucleus—are in accordance with levels of CRF_1 mRNA expression and CRH receptor binding in this nucleus (De Souza, 1987; Potter et al., 1994; Chalmers et al., 1995; Avishai-Eliner et al., 1996).

CRF_1-LI was localized to regions receiving CRH-containing projections from the amygdala. Indeed, the amygdala is considered an origin of major CRH-containing pathways, emanating from the ACe, the major output nucleus for amygdaloid projections to the brainstem and hypothalamus (Swanson et al., 1983; Sakanaka et al., 1986; Gray and Bingaman, 1996; Pitkänen et al., 1997). CRH neurons in ACe have been shown to project to the bed nucleus of the stria terminalis (BNST), lateral hypothalamus, midbrain central gray, parabrachial

nucleus, mesencephalic nucleus of the trigeminal nerve, mesencephalic reticular formation, solitary tract nucleus, and vagal nucleus (Veening et al., 1984; Sakanaka et al., 1986; Moga et al., 1989). In view of the widespread CRH projections from the ACe, it is not surprising that abundant CRF_1-LI-expressing neurons are observed in the current study. Indeed, the distribution of CRF_1-LI-labeled neurons demonstrated in this study highly overlaps that of target regions of CRH-expressing projections from the ACe. An additional CRH-expressing group of projection neurons originates in the amygdaloid corticomedial nucleus, innervating the VMH (Sakanaka et al., 1986). Accordingly, the current study demonstrated numerous CRF_1-LI-labeled neurons in VMH.

CRF_1-LI-positive neurons were abundant in most cholinergic nuclei of the basal forebrain, including the septum and the diagonal band of Broca. Interestingly, we found high levels of CRF_1-LI in both the lateral and medial septum, whereas reports on the distribution of CRF_1 mRNA have suggested a preferential localization to the medial septum (Chalmers et al., 1995). In addition, within the lateral septum, regional differences were evident in the cellular pattern of CRF_1-ir, implying regional specificity in the localization and perhaps physiological functions of this receptor. Thus, the demonstration of CRF_1-LI-positive neurons in cholinergic nuclei afferent to the hippocampal formation may suggest that the receptor participates in modulation of cholinergic input to the hippocampus.

The current study demonstrated a rich array of CRF_1-LI-expressing neurons in the hippocampal formation. CRH has been shown to influence directly synaptic function in hippocampal CA1 (Aldenhoff et al., 1983; Smith and Dudek, 1994) and CA3 (Hollrigel et al., 1998) and to excite hippocampal neurons both in vivo (Baram et al., 1997) and in vitro (Aldenhoff et al., 1983; Smith and Dudek, 1994; Hollrigel et al., 1998). These effects may be important in modulating learning and memory processes (Liang and Lee, 1988; Lee et al., 1993; Behan et al., 1995). Furthermore, recent evidence indicates that at least some of these direct effects of CRH on hippocampal neurons are mediated by CRF_1 (Baram et al., 1997).

In the absence of CRH-containing afferent projections to the hippocampus, the endogenous ligand for CRF_1—shown here to reside primarily on pyramidal layer neurons—is likely to be CRH found in local hippocampal interneurons, as described by Swanson et al. (1983) and Sakanaka et al. (1987). Recently most of these neurons have been found to be basket and chandelier cells, synapsing on soma and axon initial segment of pyramidal neurons, respectively (Yan et al., 1998b). Thus, local CRH-expressing interneurons are the likely source of ligand activating the abundant CRF_1-LI on hippocampal pyramidal layer neurons. This study documented a particularly striking density and intensity of CRF_1 immunoreactivity in CA3 pyramidal neurons. In this context, it is interesting to note that the excitatory and particularly the excitotoxic effects of CRH are maximal on CA3 hippocampal neurons (Baram and Ribak, 1995; Ribak and Baram, 1996).

In the hypothalamus, the current study demonstrated an abundant population of generally intense CRF_1-LI labeling of neurons in the PVN, VMH, and supraoptic and arcuate nuclei. While a small proportion (about 24%; 96 of 398) of PVN magnocellular neurons showed faint CRF_1-LI, parvocellular neurons were very intensely labeled. Of these, most were concentrated in the anterior, medial, and lateral parts of the parvocellular division (Swanson and Kuypers, 1980; Swanson et al., 1983). Previous studies have demonstrated that CRH-expressing parvocellular neurons of the dorsomedial division of PVN give rise to the pathway terminating in the external zone of the median eminence (Swanson et al., 1987; reviewed in Sawchenko and Swanson, 1990) that controls the release of ACTH from the pituitary. These CRH neurons thus participate in the control of ACTH release from the anterior pituitary, a key neuroendocrine component of the response to stress. In addition to this stress axis-related role, subpopulations of PVN CRH neurons, such as those residing in

the medial and lateral parvocellular regions, project to autonomic cell groups in the brainstem and spinal cord (Sawchenko, 1987). The current study documents the presence of CRF_1-LI in PVN regions containing both neuroendocrine and autonomic-projecting cells. These receptors may thus be positioned to modulate both the neuroendocrine and autonomic functions of CRH.

The current study demonstrates a striking abundance of CRF_1-LI in the PVN. This may be contrasted with previous in situ hybridization studies, showing unexpectedly little CRF_1 mRNA expression in the PVN of unstressed rats (Potter et al., 1994; Chalmers et al., 1995; Avishai-Eliner et al., 1996). However, CRF_1 mRNA levels were highly increased by stressful manipulations (Luo et al., 1994; Rivest et al., 1995; Imaki et al., 1996; Hatalski et al., 1998), as well as by intracere-broventricular administration of CRH. The current study demonstrated CRF_1-LI in parvocellular neurons from hypothalami of animals obtained under relatively stress-free circumstances (see Materials and Methods). This indicates that high CRF_1 protein levels may exist concurrent with modest steady-state CRF_1 mRNA levels. This is consistent both with a long half-life of CRF_1 and with regulation of receptor levels at the protein level. Because receptor binding studies have generally demonstrated modest levels of CRH binding in the PVN (De Souza and Kuhar, 1986), our data may suggest increased sensitivity of the immunocytochemical approach. In agreement with our results, Radulovic et al. (1998) recently reported the presence of CRF_1-ir neurons in PVN of both rat and mouse.

It should be noted that it is unlikely that the CRF_1-LI observed in this study was a result of cross-reactivity with CRF_2. Substantial homology exists between CRF_1 and CRF_2 proteins, and the immunogenic epitope used to generate the antiserum used here shares 17 of 20 amino acids with the C-terminus of CRF_2. However, Western blotting at high antiserum concentration of mouse brain of several strains revealed a single band. In addition, the overall distribution of CRF_1-ir in the current study matched that reported for CRF_1 binding and mRNA, and not that of CRF_2. Finally, using the antiserum on mouse heart, known to express CRF_2 but not CRF_1, no immunoreactivity was evident, again strongly suggesting that the antiserum does not recognize CRF_2.

In the present study, neurons strongly labeled for CRF_1-LI were also evident in the supraoptic nucleus. In view of the association of such neurons with CRH-expressing cells in PVN (vide supra), it is notable that a subset of supraoptic nucleus neurons have been shown to synthesize CRH (Kawata, 1983). CRF_1-LI was abundant in both the dorsomedial and ventromedial VMH. At the mRNA level, CRF_1 expression in the VMH has been found to be low compared with that of CRF_2 in both adult and immature animals (Chalmers et al., 1995; Eghbal-Ahmadi et al., 1998). The VMH functions to regulate food intake and energy balance. In addition, it is involved with integrating inputs from the HPA-axis, circadian rhythm, and sensory relay centers (Lovenberg et al., 1995; Eghbal-Ahmadi et al., 1999). However, the relative roles of CRF_1 and CRF_2 in mediating the effects of CRH and similar ligands in the VMH are not fully understood. The relatively high levels of VMH CRF_1-LI found in this study suggest that this receptor may participate in mediating some of the effects of CRH (and related ligands) in this region.

CRF_1-LI was abundant in monoaminergic cell groups such as the locus coeruleus, raphe, ventral tegmentum, and substantia nigra. Of these, the locus coeruleus has been shown to contain CRH-expressing neurons and fibers. A number of studies have suggested that CRH may function as a neurotransmitter in this region, involved with central integration of autonomic, behavioral, and anxiogenic effects of stressful stimuli (Valentino et al., 1992; Lehnert et al., 1998). For example, CRH injected into the rodent locus coeruleus produces an anxiogenic response (Owens and Nemeroff, 1993). In this regard, the present study

provides an anatomical basis for the involvement of the locus ceruleus CRF_1 in mediating anxiety-related effects of CRH.

CRF_1-LI was abundant in cerebellar circuits. CRH has been localized to cerebellar mossy fiber projections originating in vestibular-related brainstem nuclei (Cha and Foote, 1988; Cummings et al., 1994) and to the climbing fibers and their origin, the inferior olive (Young et al., 1986; Cummings et al., 1994; Chang et al., 1996). In accordance with the functional role of CRH as a cerebellar neurotransmitter, previous studies have demonstrated the expression of CRF_1 and CRF_2 mRNAs in the molecular and granular layers, sites of termination of climbing and mossy fibers, respectively (Potter et al., 1994; Chalmers et al., 1995). In the present study, almost all Purkinje cells showed intense CRF_1-LI, whereas these levels were generally low in both molecular and granular layers. Thus, whereas the current immunocytochemical data correlate with mRNA distribution in Purkinje cells (Chalmers et al., 1995; King et al., 1997), the current study shows low CRF_1-LI levels in the granular layer, considered rich in CRF_1 mRNA. This apparent discrepancy may be due to the synthesis of CRF_1 within cell bodies located in the granular layer and transport of the protein away from the soma, located in the granular layer, resulting in low signal intensity in this layer (Table 3).

The current study focused on CRF_1 detection in the mouse brain; the distribution may differ from that in rat. Thus, Radulovic et al. (1998) reported significant, although mainly quantitative, species differences in the distribution of the receptor between the rat and mouse. Compared with the rat, the mouse was found to express less CRF_1 protein in the neocortex and basal amygdala and significantly larger amounts of CRF_1 protein in several subcortical regions including the substantia nigra, central gray, red and Darkschewitsch nuclei, and pontine reticular nuclei.

In summary, the present immunocytochemical study reveals that the CRF_1-LI is widely yet selectively expressed in the mouse brain and that its localization generally overlaps target regions of CRH projections. In addition, CRF_1-LI distribution is generally congruent with previously published data on CRF_1 mRNA expression. However, discrepancies do exist in several regions including the central amygdaloid nucleus, septum, locus coeruleus, certain hypothalamic nuclei, and the cerebellar granular layer. These, as discussed above, may be due to differential regulation of receptor transcription and protein, to protein transport, to the cellular detail afforded by the current study, or to the presence of as yet undiscovered or cross-reacting ligands and receptors, respectively.

Abbreviations

3	principal oculomotor nucleus
3V	third ventricle
7	facial nucleus
10	dorsal motor nucleus of vagus
12	hypoglossal nucleus
AB	accessory basal amygdaloid nucleus
aca	anterior commisure, anterior part
Acb	accumbens nucleus
ACe	central amygdaloid nucleus
AD	anterodorsal thalamic nucleus

AHy	anterior hypothalamic area
Amb	ambiguous nucleus
ap	anterior parvocellular part, paraventricular hypothalamic nucleus
Arc	arcuate hypothalamic nucleus
AV	anteroventral thalamic nucleus
Bmc	basal amygdaloid nucleus, magnocellular division
CA1–3	cornu ammonis, hippocampus
cc	corpus callosum
CC	central canal
CEl	central amygdaloid nucleus, lateral division
CEm	central amygdaloid nucleus, medial division
CL	centrolateral thalamic nucleus
COa	anterior cortical amygdaloid nucleus
d	dorsal nucleus, inferior olive
DCo	dorsal cochlear nucleus
Dk	Darkschewitsch nucleus
DPB	dorsal parabrachial nucleus
DR	dorsal raphe nucleus
DTg	dorsal tegmental nucleus
ec	external capsule
En	endopiriform nucleus
EPl	external plexiform layer of olfactory bulb
EW	accessory oculomotor nucleus
FStr	fundus striate
Gl	glomeruli
Grc	granular layer of cerebellum
GrCo	granular layer of cochlear nucleus
GrDG	granular layer of dentate gyrus
Hi	hilus of dentate gyrus
ICj	islands of Calleja
icp	inferior cerebellar peduncle
Igr	internal granular layer of olfactory bulb
IO	inferior olive
IPl	internal plexiform layer of olfactory bulb
LC	locus coeruleus
LDTg	laterodorsal tegmental nucleus

lfp	longitudinal fasiculus of pons
LH	lateral hypothalamic area
Ll	lateral amygdaloid nucleus, lateral division
Lm	lateral amygdaloid nucleus, medial division
LMol	stratum lacunosum-moleculare of hippocampus
lp	lateral parvocellular part, paraventricular hypothalamic nucleus
LRt	lateral reticular nucleus
LRtS5	lateral reticular nucleus, subtrigeminal part
LSD	lateral septal nucleus, dorsal part
LSI	lateral septal nucleus, intermediate part
LSV	lateral septal nucleus, ventral part
LTz	lateral nucleus of trapezoid body
LV	lateral ventricle
Lve	lateral vestibular nucleus
Mcd	medial amygdaloid nucleus, dorsal part of central division
Mcv	medial amygdaloid nucleus, ventral part of central division
MD	mediodorsal thalamic nucleus
ME	median eminence
Me5	mesencephalic trigeminal nucleus
MHb	medial habenular nucleus
Mi	mitral cell layer of olfactory bulb
Mo5	motor trigeminal nucleus
Mol	molecular layer of cerebellum
MolDG	molecular layer of dentate gyrus
mp	medial parvocellular part, paraventricular hypothalamic nucleus
MS	medial septal nucleus
MSO	medial superior olive
MTz	medial nucleus of trapezoid body
MVe	medial vestibular nucleus
opt	optic tract
Or	oriens layer of hippocampus
PAC	periamygdaloid nucleus
PCRt	parvocellular reticular nucleus
PGi	paragigantocellular reticular nucleus
Pir	piriform cortex
pm	posterior magnocellular part, paraventricular hypothalamic nucleus

Pn	pontine nuclei
PnC	pontine reticular nucleus, caudal
PnO	pontine reticular nucleus, oral
Pr5	principal sensory trigeminal nucleus
Pur	Purkinje cell layer
PVN	paraventricular hypothalamic nucleus
py	pyramidal tract
Py	pyramidal layer of hippocampus
PyTu	pyramidal layer of olfactory bulb
Rad	stratum radiatum of hippocampus
Rt	reticular thalamic nucleus
scp	superior cerebellar peduncle
sm	stria medullaris thalamus
SNC	substantia nigra pars compacta
SNR	substantia nigra pars reticulate
SO	supraoptic hypothalamic nucleus
sol	solitary tract
SolL	nucleus solitary tract, lateral part
SolM	nucleus solitary tract, medial part
STh	subthalamic nucleus
Su7	suprafacial nucleus
VCo	ventral cochlear nucleus
VDBV	nucleus of vertical limb of diagonal band, ventral part
VL	ventrolateral thalamic nucleus
VLL	ventral nucleus of lateral lemniscus
VM	ventromedial thalamic nucleus
VMH	ventromedial hypothalamic nucleus
VMHDM	ventromedial hypothalamic nucleus, dorsomedial part
VMHVL	ventromedial hypothalamic nucleus, ventrolateral part
VP	ventral pallidum
VPB	ventral parabrachial nucleus
VTg	ventral tegmental nucleus
ZI	zona incerta

Acknowledgments

Grant sponsor: National Institutes of Health; Grant number: NS 28912; Grant sponsor: University of California Systemwide Biotechnology Research and Education Program; Grant number: 98-02.

We thank Drs. O. Steward, A. Pitkänen, L. Seress, H. Yin, and R. Bender for their valuable comments on the manuscript.

LITERATURE CITED

Aldenhoff JB, Gruol DL, Rivier J, Vale W, Siggins GR. Corticotropin releasing factor decreases postburst hyperpolarizations and excites hippocampal neurons. Science. 1983; 221:875–877. [PubMed: 6603658]

Avishai-Eliner S, Yi SJ, Baram TZ. Developmental profile of messenger RNA for the corticotropin-releasing hormone receptor in the rat limbic system. Brain Res Dev Brain Res. 1996; 91:159–163.

Baram TZ, Hatalski CG. Neuropeptide-mediated excitability: a key triggering mechanism for seizure generation in the developing brain. TINS. 1998; 21:471–476. [PubMed: 9829688]

Baram TZ, Ribak CE. Peptide-induced infant status epilepticus causes neuronal death and synaptic reorganization. Neuroreport. 1995; 6:277–280. [PubMed: 7756609]

Baram TZ, Chalmers DT, Chen C, Koutsoukos Y, De Souza EB. The CRF_1 receptor mediates the excitatory actions of corticotropin releasing factor (CRF) in the developing rat brain: in vivo evidence using a novel, selective, non-peptide CRF receptor antagonist. Brain Res. 1997; 770:89–95. [PubMed: 9372207]

Behan DP, Heinrichs SC, Troncoso JC, Liu XJ, Kawas CH, Ling N, De Souza EB. Displacement of corticotropin releasing factor from its binding protein as a possible treatment for Alzheimer's disease. Nature. 1995; 378:284–287. [PubMed: 7477348]

Castro MG, Morrison E, Perone MJ, Brown OA, Murray CA, Ahmed I, Perkins AV, Europe-Finner G, Lowenstein PR, Linton EA. Corticotrophin-releasing hormone receptor type 1: generation and characterization of polyclonal antipeptide antibodies and their localization in pituitary cells and cortical neurones in vitro. J Neuroendocrinol. 1996; 8:521–531. [PubMed: 8843021]

Cha CI, Foote SL. Corticotropin-releasing factor in olivocerebellar climbing-fiber system of monkey (*Saimiri sciureus* and *Macaca fascicularis*): parasagittal and regional organization visualized by immunohistochemistry. J Neurosci. 1988; 8:4121–4137. [PubMed: 3263473]

Chalmers DT, Lovenberg TW, De Souza EB. Localization of novel corticotropin-releasing factor receptor (CRF_2) mRNA expression to specific subcortical nuclei in rat brain: comparison with CRF_1 receptor mRNA expression. J Neurosci. 1995; 15:6340–6350. [PubMed: 7472399]

Chang CP, Pearse RVII, O'Connell S, Rosenfeld MG. Identification of a seven trans-membrane helix receptor for corticotropin-releasing factor and sauvagine in mammalian brain. Neuron. 1993; 11:1187–1195. [PubMed: 8274282]

Chang D, Yi SJ, Baram TZ. Developmental profile of corticotropin releasing hormone messenger RNA in the rat inferior olive. Int J Dev Neurosci. 1996; 14:69–76. [PubMed: 8779310]

Chen R, Lewis KA, Perrin MH, Vale WW. Expression cloning of a human corticotropin-releasing-factor receptor. Proc Natl Acad Sci USA. 1993; 90:8967–8971. [PubMed: 7692441]

Chen YC, Chen QS, Lei JL, Wang SL. Physical training modifies the age-related decrease of GAP-43 and synaptophysin in the hippocampal formation in C57BL/6J mouse. Brain Res. 1998a; 806:238–245. [PubMed: 9739145]

Chen YC, Lei JL, Chen QS, Wang SL. Effect of physical training on the age-related changes of acetylcholinesterase-positive fibers in the hippocampal formation and parietal cortex in the C57BL/6J mouse. Mech Ageing Dev. 1998b; 102:81–93. [PubMed: 9663794]

Conti LH, Foote SL. Effects of pretreatment with corticotropin-releasing factor on the electrophysiological responsivity of the locus coeruleus to subsequent corticotropin-releasing factor challenge. Neuroscience. 1995; 69:209–219. [PubMed: 8637619]

Cummings SL, Young WS III, King JS. Early development of cerebellar afferent systems that contain corticotropin-releasing factor. J Comp Neurol. 1994; 350:534–549. [PubMed: 7890829]

De Souza EB. Corticotropin-releasing factor receptors in the rat central nervous system: characterization and regional distribution. J Neurosci. 1987; 7:88–100. [PubMed: 3027279]

De Souza EB, Kuhar MJ. Corticotropin-releasing factor receptors in the pituitary gland and central nervous system: methods and overview. Methods Enzymol. 1986; 124:560–590. [PubMed: 3012254]

De Souza EB, Insel TR, Perrin MH, Rivier J, Vale WW, Kuhar MJ. Corticotropin-releasing factor receptors are widely distributed within the rat central nervous system: an autoradiographic study. J Neurosci. 1985; 5:3189–3203. [PubMed: 3001239]

Dolorfo CL, Amaral DG. Entorhinal cortex of the rat: organization of intrinsic connections. J Comp Neurol. 1998; 398:49–82. [PubMed: 9703027]

Eghbal-Ahmadi M, Hatalski CG, Lovenberg TW, Avishai-Eliner S, Chalmers DT, Baram TZ. The developmental profile of the corticotropin releasing factor receptor (CRF_2) in rat brain predicts distinct age-specific functions. Brain Res Dev Brain Res. 1998; 107:81–90.

Eghbal-Ahmadi M, Avishai-Eliner S, Hatalski CG, Baram TZ. Differential regulation of the expression of corticotropin-releasing factor receptor type 2 (CRF_2) in hypothalamus and amygdala of the immature rat by sensory input and food intake. J Neurosci. 1999; 19:3982–3991. [PubMed: 10234028]

Ehlers CL, Henriksen SJ, Wang M, Rivier J, Vale W, Bloom FE. Corticotropin releasing factor produces increases in brain excitability and convulsive seizures in rats. Brain Res. 1983; 278:332–336. [PubMed: 6605787]

Gray TS, Bingaman EW. The amygdala: corticotropin-releasing factor, steroids, and stress. Crit Rev Neurobiol. 1996; 10:155–168. [PubMed: 8971127]

Grigoriadis DE, Lovenberg TW, Chalmers DT, Liaw C, De Souza EB. Characterization of corticotropin-releasing factor receptor subtypes. Ann NY Acad Sci. 1996; 780:60–80. [PubMed: 8602740]

Hatalski CG, Guirguis C, Baram TZ. Corticotropin releasing factor mRNA expression in the hypothalamic paraventricular nucleus and the central nucleus of the amygdala is modulated by repeated acute stress in the immature rat. J Neuroendocrinol. 1998; 10:663–669. [PubMed: 9744483]

Hollrigel GS, Chen K, Baram TZ, Soltesz I. The pro-convulsant actions of corticotropin-releasing hormone in the hippocampus of infant rats. Neuroscience. 1998; 84:71–79. [PubMed: 9522363]

Imaki J, Imaki T, Vale W, Sawchenko PE. Distribution of corticotropin-releasing factor mRNA and immunoreactivity in the central auditory system of the rat. Brain Res. 1991; 547:28–36. [PubMed: 1713530]

Imaki T, Naruse M, Harada S, Chikada N, Imaki J, Onodera H, Demura H, Vale W. Corticotropin-releasing factor up-regulates its own receptor mRNA in the paraventricular nucleus of the hypothalamus. Brain Res Mol Brain Res. 1996; 38:166–170. [PubMed: 8737681]

Kawata M, Hashimoto K, Takahara J, Sano Y. Immunohistochemical identification of neurons containing corticotropin-releasing factor in the rat hypothalamus. Cell Tissue Res. 1983; 230:239–246. [PubMed: 6342798]

King JS, Madtes P Jr, Bishop GA, Overbeck TL. The distribution of corticotropin-releasing factor (CRF), CRF binding sites and CRF_1 receptor mRNA in the mouse cerebellum. Prog Brain Res. 1997; 114:55–66. [PubMed: 9193138]

Kostich WA, Chen A, Sperle K, Largent BL. Molecular identification and analysis of a novel human corticotropin-releasing factor (CRF) receptor: the CRF_2gamma receptor. Mol Endocrinol. 1998; 12:1077–1085. [PubMed: 9717834]

Lee EH, Lee CP, Wang HI, Lin WR. Hippocampal CRF, NE, and NMDA system interactions in memory processing in the rat. Synapse. 1993; 14:144–153. [PubMed: 7687386]

Lehnert H, Schulz C, Dieterich K. Physiological and neurochemical aspects of corticotropin-releasing factor actions in the brain: the role of the locus coeruleus. Neurochem Res. 1998; 23:1039–1052. [PubMed: 9704593]

Liang KC, Lee EH. Intra-amygdala injections of corticotropin releasing factor facilitate inhibitory avoidance learning and reduce exploratory behavior in rats. Psychopharmacology. 1988; 96:232–236. [PubMed: 3148150]

Lovenberg TW, Liaw CW, Grigoriadis DE, Clevenger W, Chalmers DT, De Souza EB, Oltersdorf T. Cloning and characterization of a functionally distinct corticotropin-releasing factor receptor subtype from rat brain. Proc Natl Acad Sci USA. 1995; 92:836–840. [PubMed: 7846062]

Luo X, Kiss A, Makara G, Lolait SJ, Aguilera G. Stress-specific regulation of corticotropin releasing hormone receptor expression in the paraventricular and supraoptic nuclei of the hypothalamus in the rat. J Neuroendocrinol. 1994; 6:689–696. [PubMed: 7894472]

Moga MM, Saper CB, Gray TS. Bed nucleus of the stria terminalis: cyto-architecture, immunohistochemistry, and projection to the parabrachial nucleus in the rat. J Comp Neurol. 1989; 283:315–332. [PubMed: 2568370]

Muglia L, Jacobson L, Dikkes P, Majzoub JA. Corticotropin-releasing hormone deficiency reveals major fetal but not adult glucocorticoid need. Nature. 1995; 373:427–432. [PubMed: 7830793]

Owens MJ, Nemeroff CB. The role of corticotropin-releasing factor in the pathophysiology of affective and anxiety disorders: laboratory and clinical studies. Ciba Found Symp. 1993; 172:296–308. [PubMed: 8491091]

Palchaudhuri MR, Wille S, Mevenkamp G, Spiess J, Fuchs E, Dautzenberg FM. Corticotropin-releasing factor receptor type 1 from *Tupaia belangeri*—cloning, functional expression and tissue distribution. Eur J Biochem. 1998; 258:78–84. [PubMed: 9851694]

Paxinos, G.; Watson, C. The rat brain in stereotaxic coordinates. New York: Academic Press; 1982.

Perrin MH, Donaldson CJ, Chen R, Lewis KA, Vale WW. Cloning and functional expression of a rat brain corticotropin releasing factor (CRF) receptor. Endocrinology. 1993; 133:3058–3061. [PubMed: 8243338]

Pitkänen A, Savander V, LeDoux JE. Organization of intra-amygdaloid circuitries in the rat: an emerging framework for understanding functions of the amygdala. TINS. 1997; 20:517–523. [PubMed: 9364666]

Potter E, Sutton S, Donaldson C, Chen R, Perrin M, Lewis K, Sawchenko PE, Vale W. Distribution of corticotropin-releasing factor receptor mRNA expression in the rat brain and pituitary. Proc Natl Acad Sci USA. 1994; 91:8777–8781. [PubMed: 8090722]

Powers RE, DeSouza EB, Walker LC, Price DL, Vale WW, Young WS. Corticotropin-releasing factor as a transmitter in the human olivocerebellar pathway. Brain Res. 1987; 415:347–352. [PubMed: 2886191]

Radulovic J, Sydow S, Spiess J. Characterization of native corticotropin-releasing factor receptor type 1 in the rat and mouse central nervous system. J Neurosci Res. 1998; 54:507–521. [PubMed: 9822161]

Ribak CE, Baram TZ. Selective death of hippocampal CA3 pyramidal cells with mossy fiber afferents after CRH-induced status epilepticus in infant rats. Brain Res Dev Brain Res. 1996; 91:245–251.

Rivest S, Laflamme N, Nappi RE. Immune challenge and immobilization stress induce transcription of the gene encoding the CRF receptor in selective nuclei of the rat hypothalamus. J Neurosci. 1995; 15:2680–2695. [PubMed: 7722622]

Sakanaka M, Shibasaki T, Lederis K. Distribution and efferent projections of corticotropin-releasing factor-like immunoreactivity in the rat amygdaloid complex. Brain Res. 1986; 382:213–238. [PubMed: 2428439]

Sakanaka M, Shibasaki T, Lederis K. Corticotropin releasing factorlike immunoreactivity in the rat brain as revealed by a modified cobalt-glucose oxidase-diaminobenzidine method. J Comp Neurol. 1987; 260:256–298. [PubMed: 3497182]

Sanchez MM, Young LJ, Plotsky PM, Insel TR. Autoradiographic and in situ hybridization localization of corticotropin-releasing factor 1 and 2 receptors in nonhuman primate brain. J Comp Neurol. 1999; 408:365–377. [PubMed: 10340512]

Sawchenko PE. Evidence for differential regulation of corticotropin-releasing factor and vasopressin immunoreactivities in parvocellular neurosecretory and autonomic-related projections of the paraventricular nucleus. Brain Res. 1987; 437:253–263. [PubMed: 3325130]

Sawchenko PE, Swanson LW. Localization, colocalization, and plasticity of corticotropin-releasing factor immunoreactivity in rat brain. Fed Proc. 1985; 44:221–227. [PubMed: 2981743]

Sawchenko, PE.; Swanson, LW. Organization of CRF immunoreactive cells and fibers in the rat brain: immunohistochemical studies. In: De Souza, EB.; Nemeroff, CB., editors. Corticotropin-releasing factor: basic and clinical studies of a neuropeptide. Boca Raton, FL: CRC Press; 1990. p. 29-46.

Sawchenko PE, Imaki T, Potter E, Kovacs K, Imaki J, Vale W. The functional neuroanatomy of corticotropin-releasing factor. Ciba Found Symp. 1993; 172:5–21. [PubMed: 8491094]

Sawchenko PE, Brown ER, Chan RK, Ericsson A, Li HY, Roland BL, Kovacs KJ. The paraventricular nucleus of the hypothalamus and the functional neuroanatomy of visceromotor responses to stress. Prog Brain Res. 1996; 107:201–222. [PubMed: 8782521]

Sidman, RL.; Angevine, JB.; Pierce, ET. Atlas of the mouse brain and spinal cord. Cambridge, MA: Harvard University Press; 1971.

Siggins GR, Gruol D, Aldenhoff J, Pittman Q. Electrophysiological actions of corticotropin-releasing factor in the central nervous system. Fed Proc. 1985; 44:237–242. [PubMed: 3155696]

Smith BN, Dudek FE. Age-related epileptogenic effects of corticotropin-releasing hormone in the isolated CA1 region of rat hippocampal slices. J Neurophysiol. 1994; 72:2328–2333. [PubMed: 7884462]

Swanson LW, Kuypers HG. The paraventricular nucleus of the hypothalamus: cyto-architectonic subdivisions and organization of projections to the pituitary, dorsal vagal complex, and spinal cord as demonstrated by retrograde fluorescence double-labeling methods. J Comp Neurol. 1980; 194:555–570. [PubMed: 7451682]

Swanson LW, Sawchenko PE, Rivier J, Vale WW. Organization of ovine corticotropin-releasing factor immunoreactive cells and fibers in the rat brain: an immunohistochemical study. Neuroendocrinology. 1983; 36:165–186. [PubMed: 6601247]

Swanson LW, Sawchenko PE, Lind RW. Regulation of multiple peptides in CRF parvo-cellular neurosecretory neurons: implications for the stress response. Prog Brain Res. 1986; 68:169–190. [PubMed: 3550889]

Swanson LW, Sawchenko PE, Lind RW, Rho JH. The CRH motoneuron: differential peptide regulation in neurons with possible synaptic, paracrine, and endocrine outputs. Ann NY Acad Sci. 1987; 512:12–23. [PubMed: 3327422]

Uryu K, Okumura T, Shibasaki T, Sakanaka M. Fine structure and possible origins of nerve fibers with corticotropin-releasing factorlike immunoreactivity in the rat central amygdaloid nucleus. Brain Res. 1992; 577:175–179. [PubMed: 1521144]

Vale W, Spiess J, Rivier C, Rivier J. Characterization of a 41-residue ovine hypothalamic peptide that stimulates secretion of corticotropin and beta-endorphin. Science. 1981; 213:1394–1397. [PubMed: 6267699]

Valentino RJ, Wehby RG. Corticotropin-releasing factor: evidence for a neurotransmitter role in the locus ceruleus during hemodynamic stress. Neuroendocrinology. 1988; 48:674–677. [PubMed: 2908000]

Valentino RJ, Page M, Van Bockstaele E, Aston-Jones G. Corticotropin-releasing factor innervation of the locus coeruleus region: distribution of fibers and sources of input. Neuroscience. 1992; 48:689–705. [PubMed: 1376457]

Veening JG, Swanson LW, Sawchenko PE. The organization of projections from the central nucleus of the amygdala to brainstem sites involved in central autonomic regulation: a combined retrograde transport-immunohistochemical study. Brain Res. 1984; 303:337–357. [PubMed: 6204716]

Vita N, Laurent P, Lefort S, Chalon P, Lelias JM, Kaghad M, Le Fur G, Caput D, Ferrara P. Primary structure and functional expression of mouse pituitary and human brain corticotrophin releasing factor receptors. FEBS Lett. 1993; 335:1–5. [PubMed: 8243652]

Weninger SC, Muglia LJ, Jacobson L, Majzoub JA. CRH-deficient mice have a normal anorectic response to chronic stress. Regul Pept. 1999; 84:69–74. [PubMed: 10535410]

Yan XX, Baram TZ, Gerth A, Schultz L, Ribak CE. Co-localization of corticotropin-releasing hormone with glutamate decarboxylase and calcium-binding proteins in infant rat neocortical interneurons. Exp Brain Res. 1998a; 123:334–340. [PubMed: 9860272]

Yan XX, Toth Z, Schultz L, Ribak CE, Baram TZ. Corticotropin-releasing hormone (CRH)-containing neurons in the immature rat hippocampal formation: light and electron microscopic features and

colocalization with glutamate decarboxylase and parvalbumin. Hippocampus. 1998b; 8:231–243. [PubMed: 9662138]

Young WS III, Walker LC, Powers RE, De Souza EB, Price DL. Corticotropin-releasing factor mRNA is expressed in the inferior olives of rodents and primates. Brain Res. 1986; 387:189–192. [PubMed: 3539260]

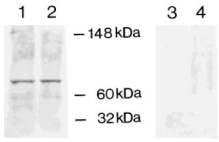

Fig. 1.

The anti-CRF_1 antiserum recognizes a single protein species, as evident from Western blot analysis. Cell lysates were prepared from mouse hypothalamus (**lanes 1** and **3**) and cerebellum (**lanes 2** and **4**). Aliquots of 50 μg protein were loaded in each lane. Following inclubation (see Materials and Methods), a single band of approximately 80 kDa was recognized by CRF_1 antiserum (1:500). Lanes 3 and 4 show that preadsorption of CRF_1 antiserum with the antigenic peptide leads to disappearance of this band.

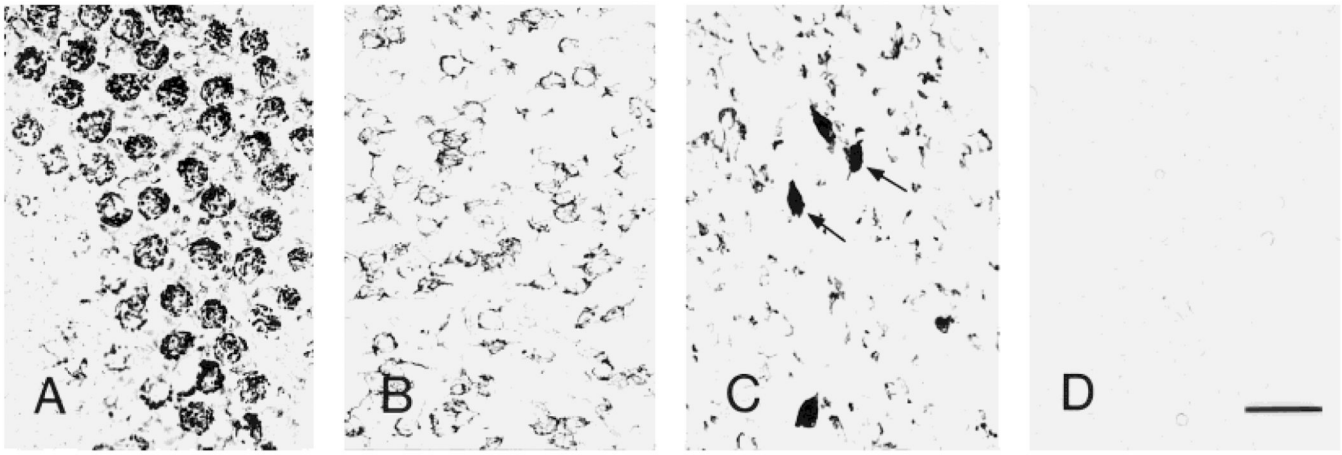

Fig. 2.

Illustration of the three principal patterns of neuronal CRF_1-like immunoreactivity (CRF_1-LI) in mouse brain. CRF_1-LI is characterized as granular (**A**, cerebellar Purkinje cells), punctate (**B**, parafascicular thalamic nucleus), or homogenous (arrows in **C**, lateral hypothalamic area). **D:** Preadsorption of the antiserum with the immunogenic epitope eliminates all the reaction signal (section shown is from thalamus). Scale bar = 40 μm (applies to A–D).

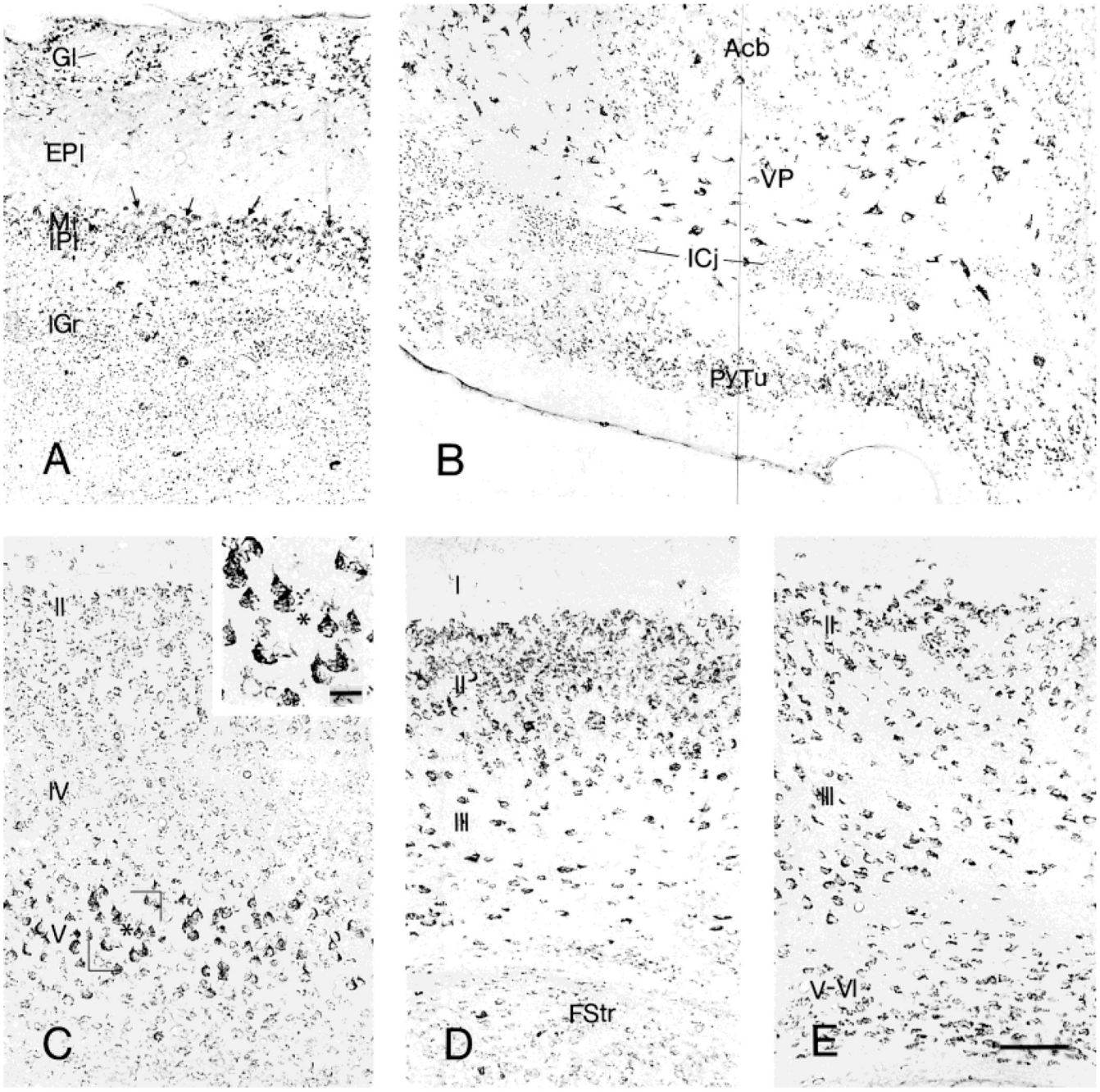

Fig. 3.

Distribution of CRF_1-like immunoreactivity in the olfactory and cortical regions: (**A**) olfactory bulb, (**B**) olfactory tubercle, (**C**) neocortex, (**D**) piriform cortex, and (**E**) entorhinal cortex. Enlargement in C shows the strongly labeled pyramidal neurons in layer V. Cortical layers are denoted by Roman numerals. Scale bars = 80 μm in E (applies to A–E); 20 μm in inset in C.

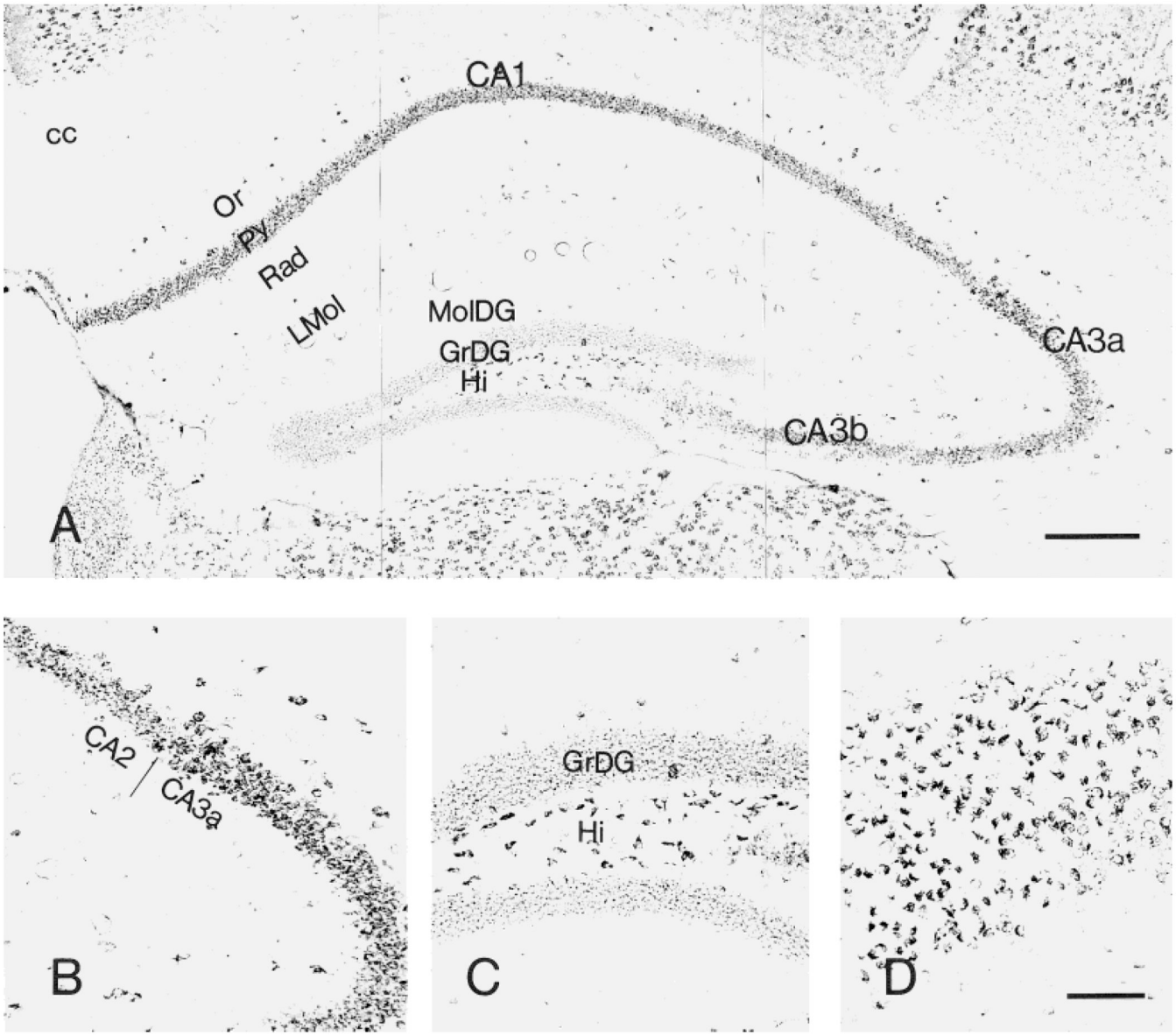

Fig. 4.

Distribution of CRF_1-like immunoreactivity in the hippocampal formation (**A**). **B:** Morphology of CRF_1-LI-expressing neurons in hippocampal CA2–3a area. **C,D:** CRF_1-like immunoreactivity in the dentate gyrus and subiculum, respectively. Within the dentate gyrus, granular cell somata are outlined by a fine mesh of weakly stained puncta, and intensely labeled neurons are present in the hilus. Most pyramidal neurons are intensely labeled in the subiculum. Scale bars = 200 μm in A; 80 μm in D (applies to B–D).

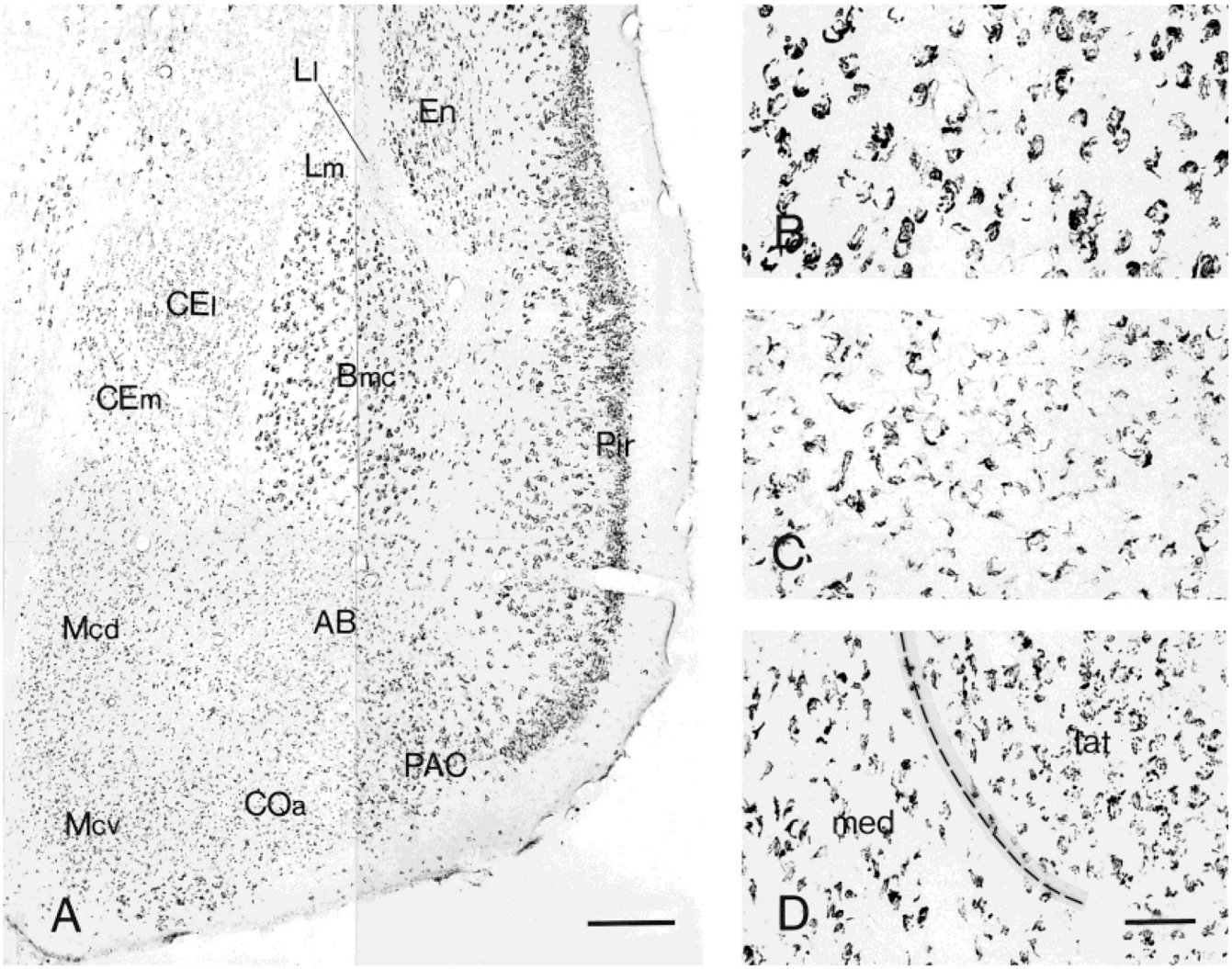

Fig. 5.

Distribution of CRF_1-like immunoreactivity in the amygdala (**A**) and the morphology of neurons showing CRF_1-LI in basal (**B**), medial (**C**), and central (**D**) nuclei. These neurons are intensely labeled throughout the magnocellular division of basal nucleus (Bmc). Within the medial nucleus (Mcd and Mcv), CRF_1 immunoreaction product frequently outlines only a portion of the cell surface. In the central nucleus, the lateral (CEl) and medial (CEm) divisions show a different staining pattern: whereas immunoreactivity in CEl consists of punctate deposits, the CEm consists of an outline of only a portion of the cell surface. Scale bars = 200 μm in A; 40 μm in D (applies to B–D).

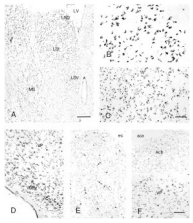

Fig. 6.

Distribution of neurons showing CRF_1-LI in septum (**A**). Higher magnification, illustrating characteristic CRF_1-ir neurons in dorsal (**B**) and lateral (**C**) septal nuclei, and in the vertical limb of the nucleus of the diagonal band of Broca (**D**). **E,F:** CRF_1-like immunoreactivity in the basal ganglia, including the accumbens nucleus (Acb) and ventral striatum (VP). Scale bars = 200 μm in A; 40 μm in C (applies to B,C); 80 μm in F (applies to D–F).

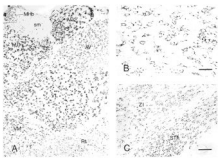

Fig. 7.

Distribution of neurons labeled for CRF_1-LI in thalamus (**A**). **B:** Higher magnification showing CRF_1-ir neurons in the nucleus reticularis. **C:** CRF_1-like immunoreactivity in the subthalamus (STh) and zona incerta (ZI). Scale bars = 40 μm in B; 80 μm in C (applies to A,C)

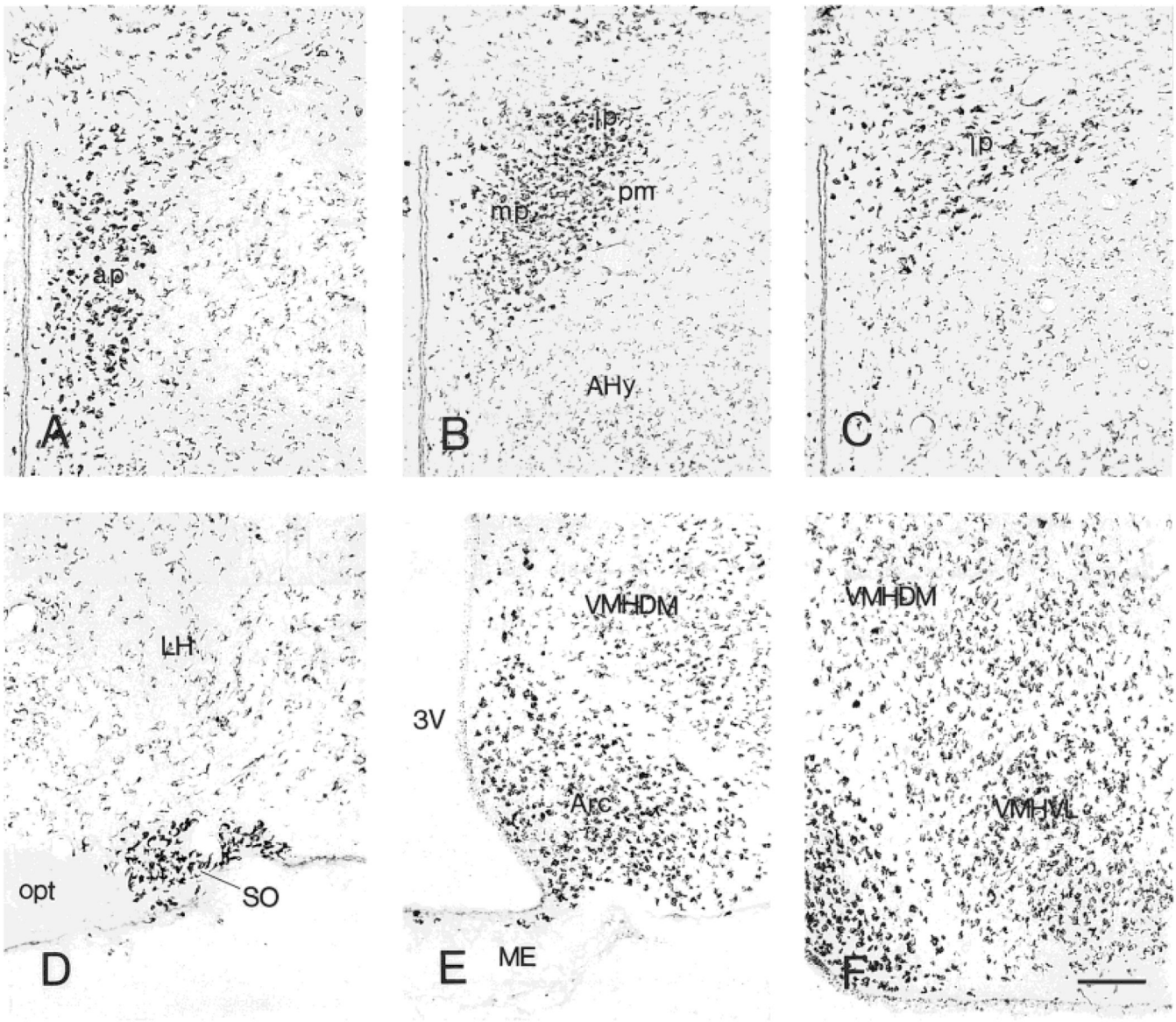

Fig. 8.

A series of coronal sections from rostral to caudal of the paraventricular nucleus, showing neurons intensely labeled for CRF_1-LI (**A–C**). Similar neurons in the supraoptic nucleus (**D**), arcuate nucleus and median eminence (**E**), and ventromedial nucleus (**F**). Scale bar = 80 μm (applies to A–F).

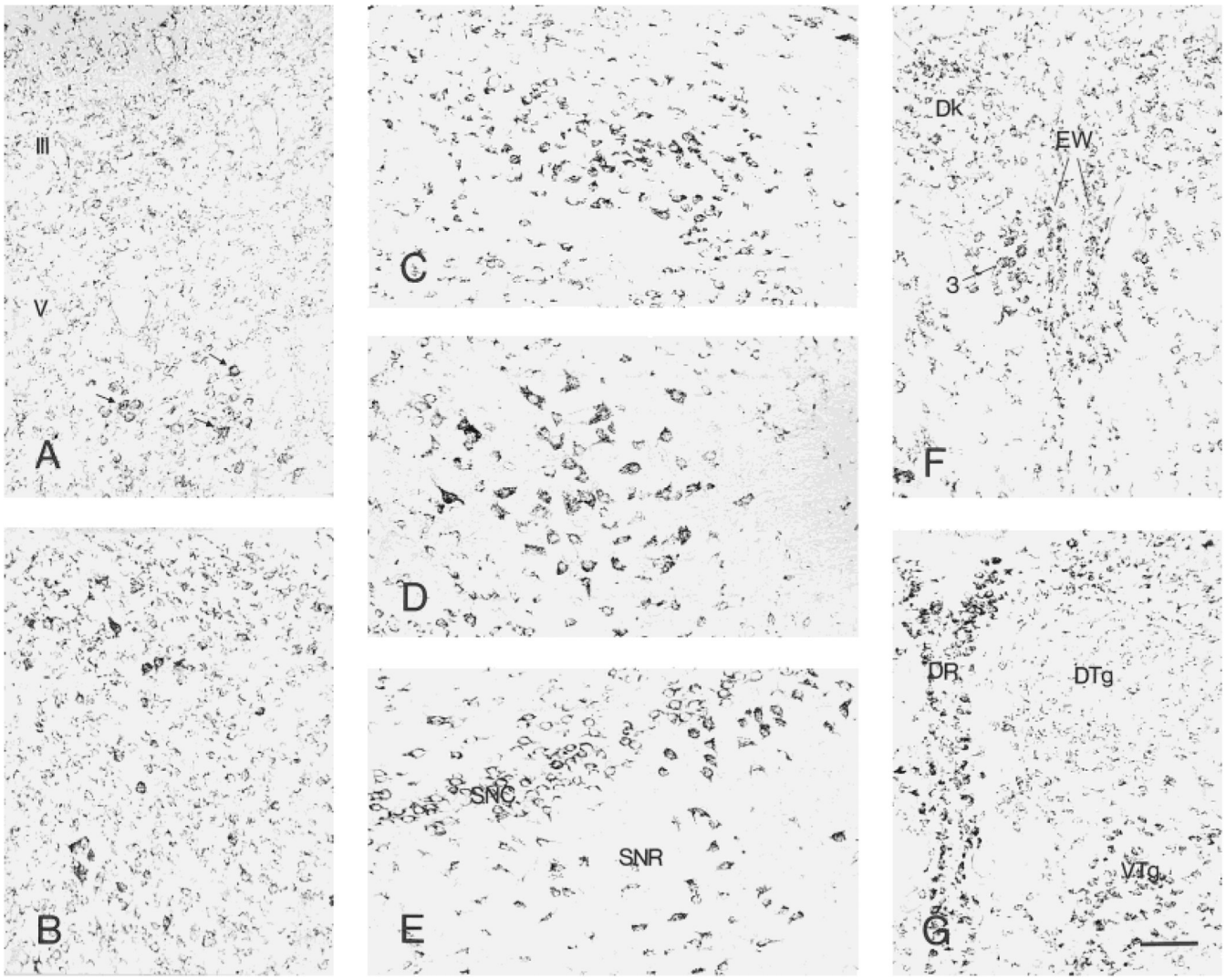

Fig. 9.

Distribution of CRF_1-like immunoreactivity in the superior (**A**) and inferior (**B**) colliculus. A few deeply labeled neurons are present in the lateral part of layer VI. In the inferior colliculus, strongly stained neurons are scattered in both the cortical and central nuclei, where most medium-sized neurons are moderately labeled. CRF_1-LI-expressing neurons in the ventral tegmental nuclei (**C**), red nucleus (**D**), and substantia nigra (**E**) are strongly labeled. The accessory oculomotor nucleus (Edinger-Westphal, **F**) is moderately or intensely labeled, whereas the dorsal raphe nucleus (**G**) is rich in highly labeled neurons. Scale bar = 80 μm (applies to A–G).

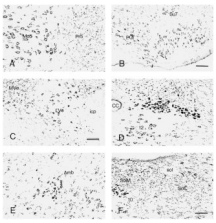

Fig. 10.

Neurons showing CRF_1-like immunoreactivity in nuclei of the trigeminal nerve (**A**), facial nucleus (**B**), vestibular nuclei (**C**), vagal dorsal motor nucleus and hypoglossal nucleus (**D**), ambiguous nucleus (**E**), and solitary tract nucleus (**F**). Scale bars = 160 μm in B,C; 80 μm in F (applies to A,D–F).

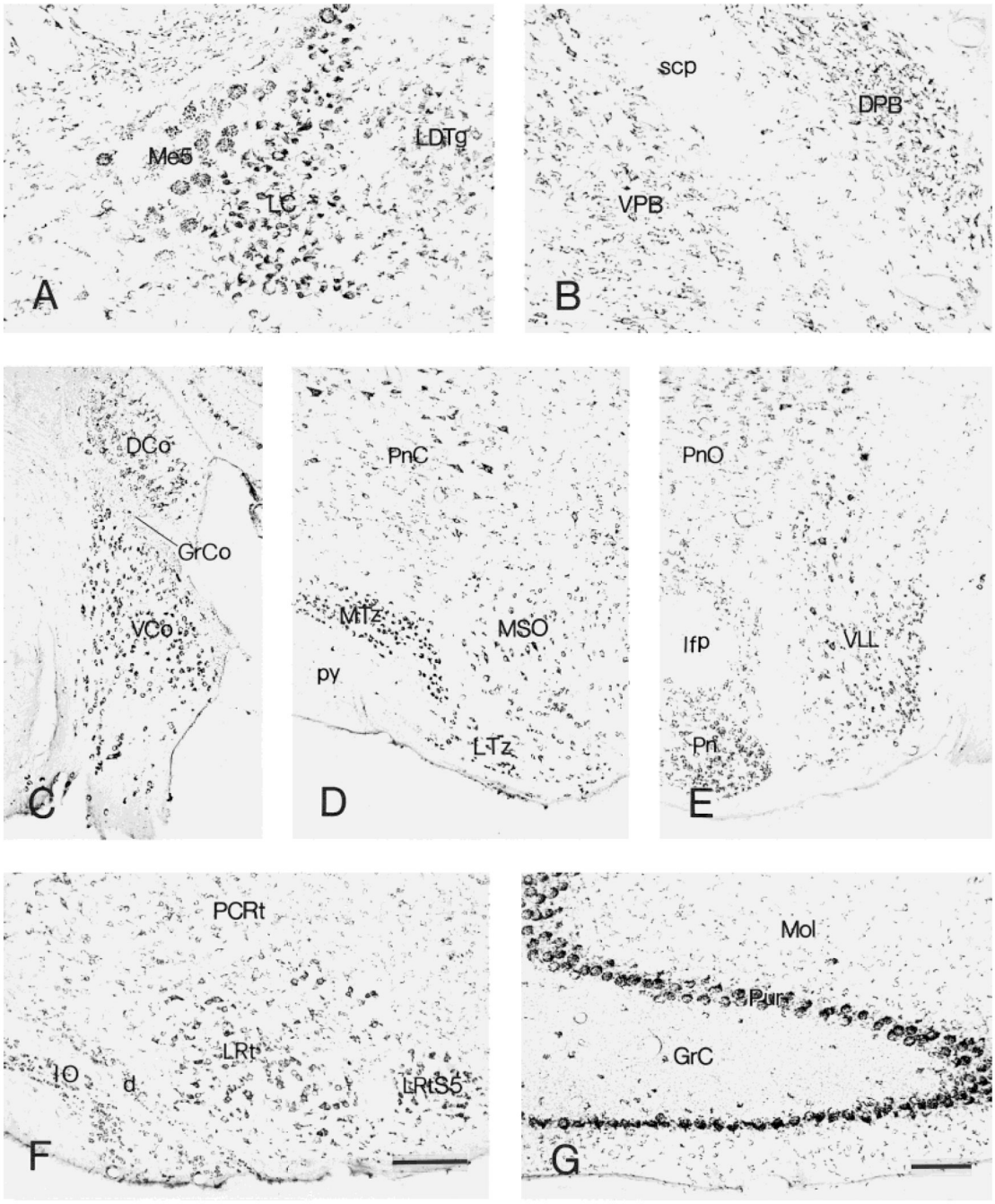

Fig. 11.

CRF_1-like immunoreactive neurons in locus coeruleus (**A**) and parabrachial nuclei (**B**). **C–E:** Distribution of labeled neurons in cochlear nuclei (C), trapezoid body (D), and ventral nucleus of lateral lemniscus (E). **F,G:** Immunoreactive neurons in the inferior olive and cerebellum, respectively. Within the cerebellum, Purkinje cells are intensely labeled. The granular layer contains scattered intensely labeled neurons, as well as numerous weakly stained fine puncta. Scale bars = 200 μm in F (applies to C–F);80 μm in G (applies to A,B,G).

TABLE 1

Distribution of Neurons Expressing CRF_1-LI in the Mouse Telencephalon: Density and Intensity

Region	Density[1]	Intensity[2]
Olfactory bulb		
Glomerular layer	++	++/+++[3]
External plexiform layer	+	+
Mitral cell layer	++++	++
Internal plexiform layer	++	++
Granular cell layer	++++	+/++
Accessory olfactory bulb		
Mitral cell layer	++++	++
Granular cell layer	++++	+/++
Olfactory tubercle		
Polymorphic layer	+++	+/++
Pyramidal layer	++++	+/++
Island of Calleja	+++	+/++
Taenia tecta	++++	++
Claustrum	++++	+/++
Endopiriform nucleus	+++	++
Neocortex		
Layer I	+	+
Layer II	++++	++
Layer III	++++	++
Layer IV	++++	+
Layer V	++++	++++
Layer VI	++++	+/++
Piriform cortex		
Layer I	+	++
Layer II	++++	++/+++
Layer III	++++	++/+++
Entorhinal cortex		
Layer IIa	++++	++/+++
Layer IIb	+++	++
Layer III	++++	++
Layers V–VI	+++	++/+++
Perirhinal cortex	++++	++
Hippocampal formation		
Hippocampus		
CA1 pyramidal layer	++++	++
CA3a pyramidal layer	++++	+++
CA3b,c pyramidal layer	++++	+/++

Region	Density[1]	Intensity[2]
Dentate gyrus		
Hilus	++	+++
Granular layer	++++	+
Molecular layer	−/+	++
Subiculum	+++	+++/++++
Amygdala		
Medial nucleus	++++	++
Cortical nucleus	++++	+/++
Central nucleus		
Medial	+++	+/++
Lateral	++++	+/++
Basal nucleus	+++	++++
Lateral nucleus	+++	+
Bed nucleus of stria terminalis		
Medical part	+++	++
Lateral part	++++	++
Basal ganglia		
Caudate-putamen	++++	+
Nucleus accumbens	++++	+/++
Fundus striati	+++	++
Globus pallidus	++	++/+++
Ventral pallidus	++	+++
Entopeduncular nucleus	++	+++
Septum		
Lateral septal nucleus	++++	+++
Medical septal nucleus	++++	++/+++
Diagonal band of Broca		
Vertical limb	+++	+++
Horizontal limb	+++	+++

[1] Density values are based on the percentage of positive cells related to total cell number. −, no positive cells; −/+, occasional cells, <10%; +, low, 10–25%; ++, moderate, 25–50%; +++, dense, 50–75%; ++++, very dense, >75%.

[2] Staining intensity: +, weakly positive; ++, moderately positive; +++, intensely positive; ++++, strongly intense.

[3] Two scores are noted because the region contains cell populations with different labeling intensity.

TABLE 2

Distribution of Neurons Expressing CRF_1-LI in the Mouse Diencephalon: Density and Intensity

Region	Density[1]	Intensity[2]
Habenula		
Medial part	++++	+++
Lateral part	++	++
Thalamus		
Anterodorsal nucleus	++	+++/++++[3]
Antroventral nucleus	+++	++
Anteromedial nucleus	+++	+++
Mediodorsal nucleus	+++	+++
Lateral dorsal nucleus	++	+++
Lateral postrior nucleus	++	+++
Ventral lateral nucleus	++	+++
Ventral postrolateral nucleus	++	+++
Ventral postromedial nucleus	++	+++
Paraventricular nucleus	+++	+++/++++
Midline nuclear group	++	++/+++
Intralaminar nuclear group	++	++/+++
Thalamic reticular nucleus	++	+/++
Hypothalamus		
Medial preoptic area	+++	+++
Lateral preoptic area	+++	++
Suprachiasmatic nucleus	+++	++
Retrochiasmatic nucleus	++	+
Supraoptic nucleus	++++	++++
Paraventricular nucleus		
Medial parvocellular division	+++	+++/++++
Magnocellular division	+	+
Ventromedial nucleus	++++	++/+++
Arcuate nucleus	++++	+++/++++
Anterior hypothalamic area	+++	++
Lateral hypothalamic area	+++	+/++
Dorsal hypothalamic area	+++	+
Dorsomedial nucleus	+++	+
Median eminence	+	+++
Subthalamic nucleus	++++	++/+++
Zona incerta	+++	+/++
Medial geniculate body	+++	+++
Lateral geniculate body	+++	++/+++

[1] Density values are based on the percentage of positive cells related to total cell number. −, no positive cells; −/+, occasional cells, <10%; +, low, 10–25%; ++, moderate, 25–50%; +++, dense, 50–75%; ++++, very dense, >75%.

[2]Staining intensity; +, weakly positive; ++, moderately positive; +++, intensely positive; ++++, strongly intense.

[3]Two scores are noted because the region contains cell populations with different labeling intensity.

TABLE 3

Distribution of Neurons Expressing CRF_1-LI in the Mouse Hindbrain: Density and Intensity

Region	Density[1]	Intensity[2]
Superior colliculus	++	+/++[3]
Inferior colliculus	++	+/++
Tegmental nuclei	+++	++/+++
Pedunculopontine nucleus	+++	+++
Red nucleus	++++[4]	+++
Substantia nigra		
Pars compacta	++	+++
Pars reticulata	++	++/+++
Raphe nuclei		
Dorsal nucleus	++	+++/++++
Median nucleus	+	++
Edinger-Westphal nucleus	+++	+/++
Principal oculomotor nucleus	+++	+++
Darkschewitsch nucleus		
Nuclei of the trigeminal nerve		
Mesencephalic nucleus	++++	+++
Motor nucleus	++++[4]	+++
Principal sensory nucleus	+++	+/++
Spinal nucleus	++	+/++
Facial nucleus	++++[4]	+++
Vestibular nuclei	+++	++/+++
Cochlear nuclei		
Dorsal nucleus	++	++
Ventral nucleus	++	+++
Vagus nucleus	++++	++++
Hypoglossal nucleus	++++	+++
Solitary nucleus	+++	+/++
Ambiguus nucleus	+++	++++
Locus coeruleus	+++	++++
Superior olive	+++	+++
Inferior olive	+++	++/+++
Nuclei of lateral lemniscus	+++	+++
Nucleus of trapezoid body		
Medial nucleus	++++	++++
Lateral nucleus	+++	++
Cerebellum		

Region	Density[1]	Intensity[2]
Molecular layer	+++	+
Purkinje cell layer	++++	++++
Granular cell layer	+++	+
Cerebellar nuclei	+++	+++

[1] Density values are based on the percentage of positive cells related to total cell number. −, no positive cells; −/+, occasional cells, <10%; +, low, 10–5%; ++, moderate, 25–50%; +++, dense, 50–75%; ++++, very dense, >75%.

[2] Staining intensity: +, weakly positive; ++, moderately positive; +++, intensely positive; ++++, strongly intense.

[3] Two scores are noted because the region contains cell populations with different labeling intensity.

[4] All large, multipolar neurons were CRF_1 immunoreactive.